

## STRUCTURAL INVESTIGATIONS OF NANOCRYSTALLINE Ti-AL AND Ni BY PAC

St. Lauer, Z. Guan, H. Wolf, and Th. Wichert

*Technische Physik, Universität des Saarlandes, D-66041 Saarbrücken, Germany*

Abstract -- Nanocrystalline Ti-Al and Ni are investigated on an atomic scale by perturbed  $\gamma\gamma$ -angular correlation spectroscopy in combination with X-ray diffraction. Ti-Al compounds produced by mechanical alloying consist of disordered solid solutions. Annealing of the samples effects a transformation into ordered intermetallic compounds, which is observed via the occurrence of characteristic electric field gradients. The local magnetic properties of nanocrystalline Ni, produced by pulsed electrodeposition, are investigated. Besides the local magnetic field known from polycrystalline Ni, a second component is detected, which is attributed to a magnetic perturbation due to grain boundaries. The width of this magnetic boundary is estimated to 3 - 4 nm.

### Introduction

The altered mechanical, diffusional [1], and magnetic [2] properties of nanocrystalline materials are intensively investigated and are compared with those of conventional polycrystals or single crystals. Here, the perturbed  $\gamma\gamma$ -angular correlation spectroscopy (PAC) is used in order to investigate the local structure of mechanically alloyed Ti-Al compounds, thereby revealing the formation of intermetallic phases. In addition, in nanocrystalline Ni the local magnetic fields within the crystallites are investigated by PAC. Ti-Al compounds are promising materials for high temperature applications because of their high melting point, low density, and good oxidation resistance [3]. The production of these compounds by mechanical alloying during ball-milling [4] aims at the improvement of the poor ductility and fracture toughness at low temperatures, which hinders their widespread use, up to now. In nanocrystalline Ni, the small grain size is accompanied by low coercitive fields resulting in improved soft magnetic properties. Especially pulsed electrodeposition (PED) offers the possibility of producing compact nanocrystalline Ni samples in large quantities at a low level of contaminations [5].

### Experimental Details

The PAC investigations were performed using radioactive  $^{111}\text{In}$  atoms decaying into  $^{111}\text{Cd}$ . The microscopic information was deduced from the local magnetic field and electric field gradient (efg). The PAC time spectrum  $R(t)$  is modulated by characteristic frequencies  $\omega_n$  as a consequence of the hyperfine interaction. In case of pure magnetic dipole interaction, two frequencies  $\omega_1 = \omega_L$  (Larmor frequency) and  $\omega_2 = 2 \omega_L$  are observed, which by the relation  $\omega_L = (\mu/I) \cdot B_{\text{loc}}$  ( $\mu = -0.7656 \mu_N$ ,  $I = 5/2 \hbar$ ) depend on the local magnetic field  $B_{\text{loc}}$  at the site of the probe nucleus. In case of pure electric quadrupole interaction ( $I = 5/2 \hbar$ ), the three frequencies  $\omega_1$ ,  $\omega_2$ , and  $\omega_3 = \omega_1 + \omega_2$  are measured, which allow the determination of the traceless efg tensor in terms of the coupling constant  $\nu_Q = e \cdot Q \cdot V_{zz} / h$  ( $Q = 0.83 \text{ b}$ ) and the asymmetry parameter  $\eta = (V_{xx} - V_{yy}) / V_{zz}$ . A detailed description of PAC can be found elsewhere [6].

Mechanical alloying was performed by milling elemental powders of Ti (purity 99.98 %) and Al (99.99 %) in a Spex 8000 ball-mill. The elemental powders were mixed in the compositions  $(1-x) \text{ Ti} + x \text{ Al}$  (with the atomic fractions  $x = 0.25, 0.50, 0.75$ ) and filled into sealed hardened steel vials. The handling of the powders and the milling were performed in a glove-box under Ar atmosphere. The radioactive  $^{111}\text{In}$  probe atoms were incorporated into Ti-Al samples by diffusion under a vacuum of  $10^{-5}$  mbar. The grain size of the nanocrystalline

samples was determined by X-ray diffraction (XRD) by analysing the broadening of the diffraction peaks [5].

The nanocrystalline Ni samples were prepared by pulsed electrodeposition [5]. Short current pulses with a length of  $t_{\text{on}} = 2$  ms and a current density of  $1 \text{ A/cm}^2$  were applied followed by an off-time of 48 ms. The used electrolyte consisted of Ni(II)sulfate (40 g/l), (K,Na)-tartrate (120 g/l), and ammonium chloride (40 g/l). The doping of Ni with  $^{111}\text{In}$  was achieved during electrodeposition by adding  $^{111}\text{InCl}_3$  to the electrolyte. As reference, polycrystalline Ni was doped with  $^{111}\text{In}$  by diffusion at 1330 K under vacuum.

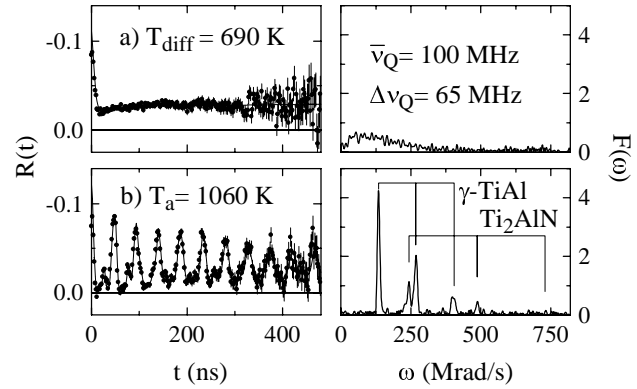


Fig. 1: PAC spectra of  $\text{Ti}_{0.50}\text{Al}_{0.50}$  after diffusion of  $^{111}\text{In}$  (a) and after annealing (b). See also Table I.

## Results and Discussion

### Ti-Al compounds

Depending on sample composition, mechanical alloying of the elemental powders leads to the formation of different homogeneous  $\text{Ti}_{1-x}\text{Al}_x$  compounds consisting of a disordered solid solution (Table I). The crystal structure is determined by XRD to be hcp ( $\text{Ti}_{0.75}\text{Al}_{0.25}$ ,  $\text{Ti}_{0.50}\text{Al}_{0.50}$ ) or fcc ( $\text{Ti}_{0.25}\text{Al}_{0.75}$ ) with a grain size of about 20 nm. For the  $\text{Ti}_{0.50}\text{Al}_{0.50}$  sample, Fig. 1a shows that after diffusion of  $^{111}\text{In}$  at  $T_{\text{diff}} = 690$  K, no unique efg is measured, which is typical for  $^{111}\text{In}$  incorporated in a disordered Ti-Al solid solution. After annealing the sample at  $T_a = 1060$  K for 16 h, however, two intermetallic compounds are formed, characterised by two well-defined efg (Fig. 1b). The first efg, characterised by  $\nu_Q = 142$  MHz and  $\eta = 0$ , indicates the formation of the equilibrium phase  $\gamma\text{-TiAl}$  [7]. The second efg, characterised by  $\nu_Q = 259$  MHz and  $\eta = 0$ , is attributed to the ordered phase  $\text{Ti}_2\text{AlN}$  [8].

Table I : Sample composition, milling-time, and crystal structure of the mechanically alloyed  $\text{Ti}_{1-x}\text{Al}_x$  samples along with the observed efg of the intermetallic compound formed after annealing.

sample	milling-time	solid solution	intermetallic compound	efg
$\text{Ti}_{0.75}\text{Al}_{0.25}$	16 h	hcp	$\alpha_2\text{-Ti}_3\text{Al}$	$\bar{\nu}_Q = 32$ MHz, $\Delta\nu_Q = 12$ MHz
$\text{Ti}_{0.50}\text{Al}_{0.50}$	13 h	hcp	$\gamma\text{-TiAl}$	$\nu_Q = 142$ MHz, $\eta = 0$
			$\text{Ti}_2\text{AlN}$	$\nu_Q = 259$ MHz, $\eta = 0$
$\text{Ti}_{0.25}\text{Al}_{0.75}$	31 h	fcc	$\tau\text{-TiAl}_3$	$\nu_Q = 101$ MHz, $\eta = 0$
			$\text{Ti}_2\text{AlN}$	$\nu_Q = 259$ MHz, $\eta = 0$

As is shown in Table I, the intermetallic compounds observed at high temperatures correspond for all three compositions to the respective equilibrium phase. The formation of  $\text{Ti}_2\text{AlN}$ , which is also observed in  $\text{Ti}_{0.25}\text{Al}_{0.75}$  samples, indicates the incorporation of N

impurities during ball-milling. The experiments on Ti-Al compounds are described in more detail elsewhere [8, 9].

### Nanocrystalline Ni

For nanocrystalline Ni, which is grown by PED, a mean grain size of 40 nm is determined by XRD. The modulation in the PAC spectrum (Fig. 2a) is caused by the magnetic dipole interaction of ferromagnetic Ni. The Larmor frequency  $\omega_L^0 = 97.6$  Mrad/s is typical of polycrystalline Ni [10] as is also confirmed in Fig. 2b and shows no measurable line broadening ( $\Delta\omega_L^0 = 0$  Mrad/s). In addition, a second, new component is observed, which is shifted to a lower frequency  $\omega_L^1 = 95.8$  Mrad/s and is significantly broadened ( $\Delta\omega_L^1 = 6$  Mrad/s). About  $f_0 = 49\%$  of the probe atoms are associated with  $\omega_L^0$  and  $f_1 = 37\%$  with the new frequency  $\omega_L^1$ . The observation of a second, shifted and broadened frequency component is similar to PAC results obtained in Ni crystals, whereby the  $^{111}\text{In}$  atoms are incorporated one or two monolayers beneath a  $\langle 111 \rangle$ -surface [11], and in polycrystalline Ni, whereby the  $^{111}\text{In}$  atoms are surrounded by non-magnetic impurities [12].

The new frequency  $\omega_L^1$  gradually disappears during annealing of the sample at temperatures between 423 K and 773 K [13]. The temperature of 423 K agrees with the temperature, at which the beginning of grain growth was observed by XRD [5]. The component  $\omega_L^1$ , therefore, is characteristic of nanocrystalline Ni and is not caused by impurities, because impurities are not expected to start to disappear after annealing of the sample at 423 K.

The local magnetic fields measured as a function of the sample temperature (Fig. 3, top) show that the component  $B_{\text{loc}}^0$ , which is derived from  $\omega_L^0$ , follows exactly the values of polycrystalline Ni [10]. The component  $B_{\text{loc}}^1$ , derived from  $\omega_L^1$ , shows the same temperature dependence, but it is shifted to lower fields. Obviously, both  $B_{\text{loc}}^0$  and  $B_{\text{loc}}^1$  are proportional to the saturation magnetisation in Ni.

The application of an external magnetic field  $B_0$  leads to a polarisation of magnetic domains in the sample. The influence on  $B_{\text{loc}}$  is shown in Fig. 3 (bottom): Almost no change occurs at small  $B_0$ , because the arising demagnetising field compensates the external field. Above  $B_0 = 0.2$  T,  $B_{\text{loc}}^0$  and  $B_{\text{loc}}^1$  start to decrease indicating negative Fermi contact fields. Above  $B_0 = 0.8$  T, a complete polarisation of the magnetic domains is visible and the local fields decrease by the amount of the additionally applied external field  $B_0$ . The dashed lines in Fig. 3 (bottom) describe the theoretically expected behaviour of  $B_{\text{loc}}$  for the demagnetized and the magnetized sample. The

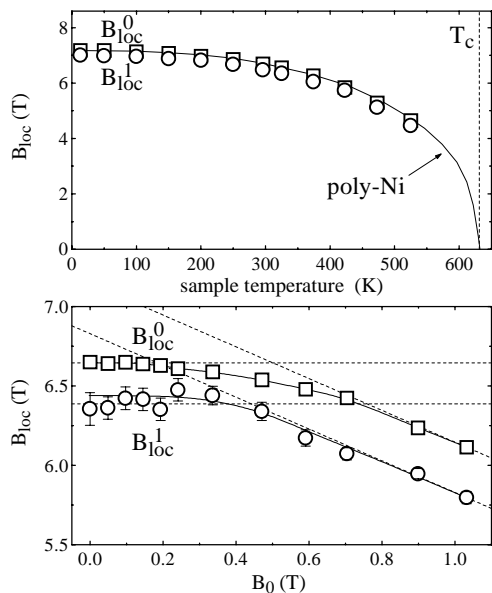


Fig. 3: The local magnetic fields  $B_{\text{loc}}^0$  and  $B_{\text{loc}}^1$  as a function of sample temperature (top) ( $T_C$ : Curie temperature) and of external magnetic field  $B_0$  (bottom). The dashed lines indicate  $B_{\text{loc}}$  in case of a demagnetized and a magnetized sample.

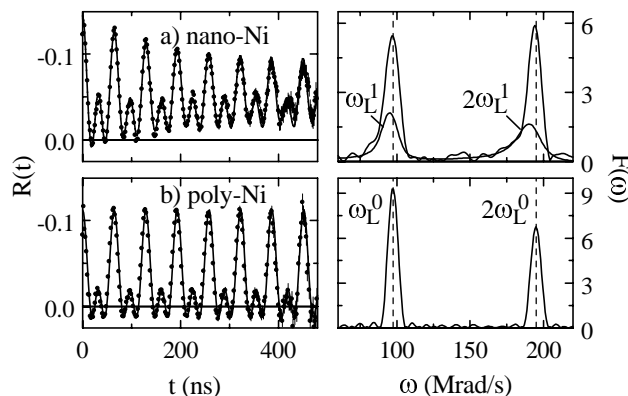


Fig. 2: PAC spectra measured in nanocrystalline (a) and in polycrystalline Ni (b) in zero external field at 295 K.

deviation of the data points from the dashed curve, which is dominated by the magnetisation process of the sample, is smaller for  $B_{loc}^1$  as for  $B_{loc}^0$ . This observation seems to indicate a modified magnetisation process for  $B_{loc}^1$  and has to be investigated more precisely in future experiments.

Based on the experimental data, a microscopic model describing the local magnetic properties of nanocrystalline Ni is proposed in Fig. 4. The component  $B_{loc}^0$  is typical of the probe atoms in the centre of Ni crystallites, whereas the component  $B_{loc}^1$  is typical of probe atoms at surface regions of the crystallites, where magnetic perturbations caused by the neighbouring grain boundaries are present. From the measured fraction  $f_1 = 37\%$ , the width of the magnetically perturbed region is estimated to  $\delta \approx 3 - 4$  nm, using the grain size of 40 nm determined by XRD and assuming a statistical distribution of the  $^{111}\text{In}$  atoms over the whole sample. As a consequence of this interpretation, the magnetic boundary turns out to be significantly larger than the crystallographic grain boundary, of which the width is estimated to about 0.5 nm [1]. The magnetic perturbation does not seem to affect the temperature dependence of the local magnetisation as shown in Fig. 3. The effect on the magnetisation in an external magnetic field has to be investigated more precisely.

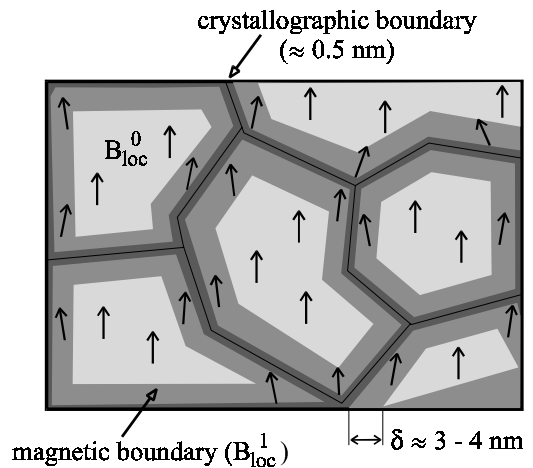


Fig. 4: Model of the local magnetic structure in nanocrystalline Ni.

### Acknowledgements

We thank M. Schmelzer, Dr. H. Natter, and Prof. Dr. Hempelmann (Saarbrücken) for the introduction to PED and XRD analysis of the Ni samples, Dr. C.E. Krill (Lehrstuhl Prof. Dr. Birringer, Saarbrücken) for the XRD analysis of the Ti-Al samples. The financial support by the Deutsche Forschungsgemeinschaft (SFB 277) is gratefully acknowledged.

### References

- [1] R.W. Siegel in Materials Science and Technology, vol. **15**, ed. R.W. Cahn, (VCH, Weinheim, 1991) p. 583
- [2] G. Herzer, Scripta Met. et Mat. **33** (1995) 1741
- [3] H.A. Lipsitt, Mat. Res. Soc. Symp. Proc. **39** (1985) 351
- [4] M. Oehring, T. Klassen, and R. Bormann, J. Mater. Res. **8** (1993) 2819
- [5] H. Natter, M. Schmelzer, and R. Hempelmann, J. Mat. Res. **13** (1998) 1186
- [6] Th. Wichert and E. Recknagel, in Microscopic Methods in Metals, ed. U. Gonser, Topics in Current Physics **40** (1986) 317
- [7] J. Fan and G.S. Collins, Hyp. Int. **79** (1993) 745
- [8] St. Lauer, Z. Guan, H. Wolf, and Th. Wichert, Materials Science Forum vol. **269-272** (1998) 485
- [9] St. Lauer, Z. Guan, H. Wolf, and Th. Wichert, submitted to J. Mater. Res.
- [10] D.A. Shirley, S.S. Rosenblum, and E. Matthias, Phys. Rev. **170** (1968) 363
- [11] J. Voigt, R. Fink, G. Krausch, B. Luckscheiter, R. Platzer, U. Wöhrmann, X.L. Ding, and G. Schatz, Phys. Rev. Lett. **64** (1990) 2202
- [12] G.S. Collins, Hyp. Int. **9** (1981) 465
- [13] St. Lauer, Z. Guan, H. Wolf, H. Natter, M. Schmelzer, R. Hempelmann, and Th. Wichert, submitted to Nanostructured Materials